Comparison of different approaches for considering vehicle-bridge-interaction in dynamic calculations of high-speed railway bridges

Lara Bettinelli [*], Bernhard Glatz, Andreas Stollwitzer, Josef Fink

TU Wien, Institute of Structural Engineering, Karlsplatz 13, 1040 Vienna, Austria

ABSTRACT

The consideration of vehicle-bridge-interaction effects can be crucial in the computational determination of realistic dynamic bridge vibrations during train crossing. In order to implement these effects into calculations with the simplified Moving Load Model, the concept of additional mass or additional damping of the bridge structure was developed. Besides normative specifications, further numerically and analytically derived approaches are now available to determine the bridge structure's additional damping value. In this numerical study, one approach for determining an additional mass and four different approaches to determine additional damping are applied to dynamic calculations of 65 railway bridges. The calculation results are compared with those obtained by applying a more sophisticated multi-body model of the train, yielding results closer to reality. All calculations are performed for two train types, a conventional locomotive-hauled Railjet and the ICE 4 with partly powered passenger cars. The comparison of results indicates that applying one of the redesigned approaches can reflect the influence of vehicle-bridge-interaction for the investigated trains significantly better than the approach according to current calculation standards. However, several application limitations due to structural and train properties were observed.

1. Introduction

The expansion of railway traffic as a highly efficient, economical, and environmentally sustainable means of transport plays a central role in achieving the overarching goal of climate neutrality. In this context, expanding the existing high-speed rail network led to several challenges for engineers and researchers aiming to preserve a well-functioning infrastructure and to enable economical operation planning. One primary goal is to computationally predict structural vibrations of railway bridges subjected to high-speed traffic as reliably as possible, with particular consideration of effects of resonance which more frequently occur in high-speed traffic.

There are various calculation models with different levels of complexity, calculation efficiency, and accuracy applicable for dynamic calculations of railway bridges. The definition of the mechanical model representing the dynamic excitation exerted by high-speed train transit proved to be an essential influencing factor on the quality of calculation results of dynamic bridge vibrations. When choosing a vehicle model,

different criteria are pursued; On the one hand, the selected vehicle models should allow the calculation of bridge vibrations as realistic as possible. On the other hand, the computational efficiency and manageability of the models should be preferably high without the need for a high number of input parameters to enable a wide range of applications.

Detailed and complex calculation models generally provide a better concordance of calculation results with the actual structural behavior. Those more detailed models require good knowledge of the trains' properties, the bridge structures, and the superstructure's dynamic behavior. Furthermore, they involve a high number of degrees of freedom at the expense of computational efficiency. The European and national standards (EN 1991–2:2003/AC:2010 [1] and national annexes) allow for dynamic calculations with strongly simplified and easily manageable models, such as the commonly adopted moving load model (MLM), which idealizes the train as a sequence of axle loads moving over the structure with constant velocity. However, the MLM cannot capture effects due to the dynamic interaction of vehicle and bridge vibrations and, thus, can yield excessive structural vibrations,

especially in the case of resonance events (among others, described in [2–6]).

More sophisticated mechanical models depicting the vehicles as multi-body systems like the detailed interaction model (DIM) can consider these, in most cases, vibration-reducing effects of vehicle-bridge-interaction (VBI) and produce more realistic results of structural vibrations. Thus, they can facilitate the computational verification of compliance with the serviceability limits specified in EN 1990:2002/A1:2005/AC:2010 [7], ensuring traffic safety. This is particularly the case for the maximum vertical structural accelerations, which are limited to 3.5 m/s^2 by [7] if no other national limit must be applied. Vertical deformations of the bridge structure are also limited to $L/600$, with L being the bridge span, but since this design criterion is generally less critical than the vertical acceleration limit, the focus of the following investigations was laid on the latter.

According to the investigations in [8], the vibration-reducing influence of the VBI on the structural accelerations correlates in particular with three parameters that can be formulated as length, mass, and frequency ratios of the bridge structure and the crossing vehicle. The influence is most pronounced when the fundamental frequency of the considered structures corresponds approximately to the bogie frequencies (the primary suspension stage), and the bridge mass is low compared to the bogie masses.

While producing more realistic and generally less critical calculation results in terms of design-relevant accelerations, more complex vehicle models require more input parameters and higher computational performance. Therefore, current research in railway bridge dynamics aims to extend simplified calculation models to depict the beneficial effects of VBI with moderate effort.

One approach is to account for the train masses resonating with the bridge structure by adding its distributed mass to the latter, as proposed in the Austrian guidelines for dynamical calculations of railway bridges [9]. This approach entails some disadvantages described in [9], such as manipulating the structures' fundamental frequencies, which makes its applicability depend on the considered structural properties.

The European standard EN 1991–2:2003/AC:2010 [1] to be adopted for dynamic calculations of railway bridges propose the so-called additional damping method to include the effects of the VBI while applying the simplified MLM. Following this method, an additional damping value dependent on the bridge span is assigned to the bridge structure. However, numerous studies show that the structural accelerations resulting from calculations according to the current standard specifications differ significantly from results obtained with more sophisticated vehicle models (see [3–5,8]). For instance, depending on considered train and bridge characteristics, the maximum bridge accelerations can either be significantly overestimated, subsequently leading to uneconomical operational planning and rehabilitation methods, or they might even yield unsafe results (see [4,5,8]).

Several alternative proposals were recently published in [10–12] to determine the additional damping, taking into account key parameters of the structure and trains to address this problem. The contributions in [10,11] present analytically derived methods to determine the additional damping factors, while the formulas given in [12] are based on the evaluation of a numerical study conducted on a fictitious parametric field of bridges and four different trains. The studies in [10–12] verify the respective methods by applying them to individual calculation examples of bridges and trains. They find good agreement between the calculated vibrations and the results obtained using a more complex vehicle model.

This contribution presents an extensive numerical study of 65 existing structures with a broad range of spans, masses, damping, and fundamental frequencies aiming to evaluate the influence of the different approaches to consider VBI by implementing an additional mass distribution or additional damping to the bridge structures and detect eventual shortcomings of each method. The effect of applying one of the recently published alternative methods in [10–12] for additional

damping on MLM calculations compared to the standard specification in [1] and the approach of additional mass according to [9] is evaluated for two high-speed trains, the Austrian Railjet and the German ICE 4. As a reference, all calculations were performed with the DIM of both trains.

This contribution aims to find answers to the following questions:

- How much do the calculation results of structural accelerations based on the MLM and the alternative formulations of additional damping differ from the reference values obtained with the DIM?
- How do the calculation results of accelerations obtained with the alternative formulation of additional damping compare to those obtained with normative specifications?
- Can a recommendation be given for applying the methods for specific structural properties?

It should be noticed that the structural model used depicts all the properties through a beam element with a limited number of considered vibration modes (see descriptions in section 2.1). Investigations in [13] have shown that with a more precise three-dimensional model of the bridge structure, significantly higher accelerations may occur in the bridge deck area due to local vibration modes in the higher frequency range of up to 30 Hz, which cannot be recorded by solely considering the global vibration modes. Moreover, the bridge model of the example examined in [13] reacted to the consideration of VBI by increased deck accelerations, in contrast to the accelerations of the main girders, which the VBI mainly reduced. Since these effects cannot be taken into account in the study presented here due to the selected computationally efficient two-dimensional modeling of the bridge structures, the following results are limited to the influence on the main structural vibration modes.

2. Mechanical models

The mechanical models of the bridge structures and vehicles used in this study are exclusively two-dimensional models whose degrees of freedom can only record vertical vibrations of the bridge structures, in contrast to more complex and computationally expensive three-dimensional models, e.g., described in [14–20]. Planar models cannot consider horizontal deformations in the transverse direction and torsional vibrations. However, the idealization using two-dimensional models is sufficiently accurate in many cases if lateral loads are not to be expected or investigated and it is a bridge structure with beam-like behavior [21]. This condition is met for the structures considered here, all designed as single-track bridges with no excentrical loading. Still, it should be pointed out that in reality, interactions between the torsional and bending vibrations can also occur, especially when the natural frequencies for both are close, as, for example, for the structure investigated in [6]. The planar modeling of the following study cannot take these interference effects into account. Furthermore, horizontal deformations in longitudinal direction, which could, for instance, occur when considering track-bridge-interaction and horizontal bearing displacements, were not considered.

2.1. Applied bridge model

The bridge structures in the numerical calculations of this paper are modeled as simply-supported single-track and single-span girders, considering bending deformations only (Bernoulli-Euler beam). The following equation of motion is derived by modal analysis:

$$\mathbf{M_B}\,\ddot{\mathbf{q}} + \mathbf{C_B}\,\dot{\mathbf{q}} + \mathbf{K_B}\,\mathbf{q} = \mathbf{p_B} \tag{1}$$

The modal mass, damping, and stiffness matrices $\mathbf{M_B}$, $\mathbf{C_B}$ and $\mathbf{K_B}$ on the left side of Eq. (1) are calculated using the span L, mass per unit length μ, bending stiffness EA_{zz}, and Lehr's damping ratio ζ (by applying Rayleigh damping) of the bridge.

The vector of eigenfunctions

$$\boldsymbol{\phi}(x) = \left[\sin\left(\frac{\pi x}{L}\right), \sin\left(\frac{2\pi x}{L}\right), \cdots, \sin\left(\frac{n\pi x}{L}\right) \right]^T \tag{2}$$

can be used to transform the time-dependent generalized displacements

$$\mathbf{q}(t) = [q_1(t), q_2(t), \cdots, q_n(t)] \tag{3}$$

and their time derivatives (velocities $\dot{\mathbf{q}}(t)$ and accelerations $\ddot{\mathbf{q}}(t)$) for n considered vibration modes into the time- and place-dependent dynamic bending deflection $w_B(x,t)$ and its time derivatives as follows:

$$w_B(x,t) \approx w_B^*(x,t) = \mathbf{q}(t)\,\boldsymbol{\phi}(x) \tag{4}$$

2.2. Applied vehicle models

The generalized load vector $\mathbf{p_B}$ in Eq. (1) depends on the applied load model. The European standard [1] prescribes dynamic calculations with the moving load model (MLM, see Fig. 1-a and section 2.2.1) though acknowledging that this very simplified excitation model cannot include the (mostly vibration-damping) effects of vehicle-bridge-interaction (VBI). According to [1], these effects can be included by using more complex vehicle models like the detailed interaction model (DIM, Fig. 1-b and section 2.2.2) or by applying additional damping to the model of the structure (see section 2.3.2). The following calculations use both models, the MLM and the DIM.

Both vehicle models assume a constant train speed and rigid and continuous contact between rail and wheelsets, the latter forming the following coupling condition in which $w_{w,i}$ is the displacement of a wheelset i at the point of contact x_i:

$$w_{w,i}(t) = w_B(x_i, t) \tag{5}$$

No track irregularities were considered in the here described studies. However, it should be noted that they can have a decisive influence on the compliance with running safety requirements, described, for example, in [18].

2.2.1. Moving load model (MLM)

In the case of the MLM consisting of m axle loads $F_{stat,i}$ representing the static contact forces of each wheelset (see Fig. 1-a), the load vector $\mathbf{p_B}$ can be defined by Eq. (6) with the rectangular function $\Gamma(x)$ to ensure that only loads located on the bridge are considered in the dynamic calculation.

$$\mathbf{p_B} = \sum_{i=1}^{m} F_{stat,i}\,\Gamma(x_i)\,\boldsymbol{\phi}(x_i) \tag{6}$$

The equation of motion of the bridge can subsequently be solved using numeric time integration methods. In the numerical studies described in the following, a differential equation solver for stiff problems (MATLAB ode15s, see [22]) based on the numerical differentiation formulas (NDFs) was used to solve the equations of motion.

2.2.2. Detailed interaction model (DIM)

In calculations using the detailed interaction model, the load vector $\mathbf{p_B}$ is extended to $\mathbf{p_B^*}$ by the dynamic force components $F_{k,i}$ and $F_{c,i}$ due

to the spring and damper elements representing the primary suspension (see Fig. 1-b) and the inertia forces of the wheelsets $m_{w,i}\ddot{w}_{w,i}(t)$:

$$\mathbf{p_B^*} = \sum_{i=1}^{m} \left[F_{stat,i} - F_{k,i}(t) - F_{c,i}(t) - m_{w,i}\,\ddot{w}_{w,i}(t) \right] \Gamma(x_i)\boldsymbol{\phi}(x_i) \tag{7}$$

Additionally, a second equation of motion (8) for the kinematics of the vehicle multi-body system connected to the equation of the bridge by the coupling condition acc. to Eq. (5) has to be solved for each time step. The properties of the car bodies, bogies, and primary and secondary suspension elements are included in the mass, damping, and stiffness matrices $\mathbf{M_V}$, $\mathbf{C_V}$ and $\mathbf{K_V}$. The vector $\mathbf{u}$ and its time derivatives $\dot{\mathbf{u}}$ and $\ddot{\mathbf{u}}$ contain six degrees of freedom for each coach, one translational, and one rotatory for each car body, respectively bogie (see Fig. 1-b).

$$\mathbf{M_V}\,\ddot{\mathbf{u}} + \mathbf{C_V}\,\dot{\mathbf{u}} + \mathbf{K_V}\,\mathbf{u} = \mathbf{F_{\dot{w}}} + \mathbf{F_w} \tag{8}$$

The load vector on the right side of Eq. (8) consists of the spring and damper forces $\mathbf{F_{\dot{w}}}$ and $\mathbf{F_w}$ acting on each bogie. More detailed information regarding both vehicle models can be found, for instance, in [23–28].

2.3. Consideration of vehicle-bridge-interaction (VBI)

This paper focuses on investigating the effects of applying one of five different methods for considering the influence of VBI in calculations with the simplified load model (MLM). These approaches are referred to as M1 to M5 and are briefly explained below.

2.3.1. M1 – Additional mass acc. to ÖBB guidelines [9]

The ÖBB guideline for dynamic calculations of railway bridges [9] provides a simple approach to considering the inertia of the train masses in MLM calculations by increasing the mass distribution μ of the examined bridge structures by $\Delta\mu_{M1} = 2\,000$ kg m^{-1}. This additional mass corresponds approximately to the average mass per unit length of a train of the high-speed load model A (HSLM-A) for passenger trains, required for dynamic analyses according to the EN 1991–2:2003/AC:2010 [1]. The size of the constant axle loads acting on the structure when applying the MLM is unchanged.

The distributed train masses generally lead to lower structural accelerations in the event of resonance due to the higher inertia forces with respect to static equilibrium. Furthermore, it reduces the fundamental bending frequencies of the examined structures, and thus the corresponding resonance velocities decrease. Consequently, calculations using this method can result in the computational occurrence of resonance events that would be observed at higher train speeds in calculations without an additional mass.

The significant reduction in the structural acceleration in the case of resonance can yield unsafe results in structures with short spans (compared to the car lengths d), usually related to relatively high fundamental frequencies n_0 where the VBI has little influence (e.g., observed in [8]. Therefore, the ÖBB guideline prescribes the additional mass to be considered only for structures exceeding 20 m span. For medium-sized structures (spans from 7 to 20 m), the calculation must be carried out with and without additional mass, and the case yielding the
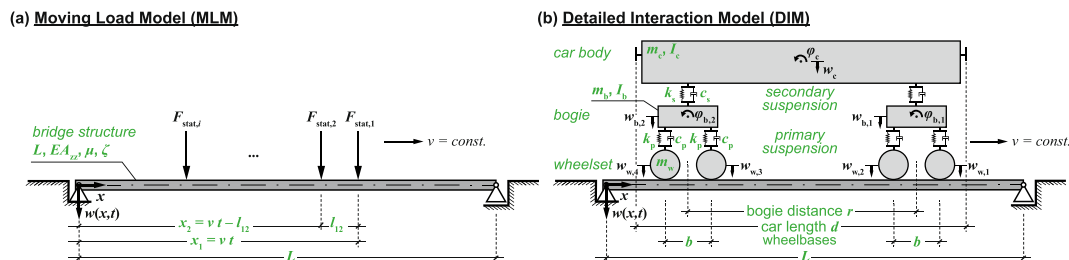
Fig. 1. Schematic representation of applied vehicle models. (a) moving load model; (b) detailed interaction model.
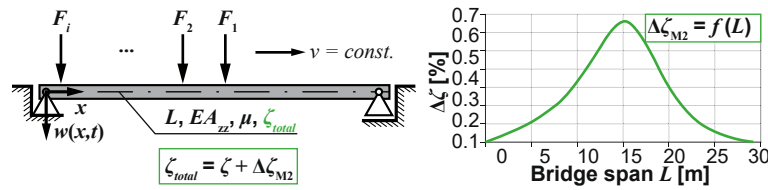
Fig. 2. M2 - span-dependent additional damping function acc. to [1].

highest accelerations shall be used for design purposes. The calculations in this paper were performed applying method M1 for all considered structures (described in section 3.2), regardless of their spans.

2.3.2. M2 - additional damping acc. to EN 1991–2:2003/AC:2010 [1]

The European design standard EN 1991–2:2003/AC:2010 [1] applying for dynamic calculations allows taking the vibration-reducing influences of VBI into account for structures with spans up to 30 m through the approach of additional damping $\Delta\zeta$ which can be added to the structural damping ratio ζ usually obtained from in–situ measurements or defined in normative specifications (see Fig. 2).

The specifications of the additional damping ratio $\Delta\zeta$ in [1] are based on comparative calculations carried out in [29] for bridge structures with spans from 5 to 30 m. The calculations in [29] use moving load models as well as multi-body models (a simplified interaction model) of two trains, the ICE 2 and the Eurostar. In the case of calculations with the moving load model, an additional damping $\Delta\zeta$ was iteratively assigned to the structure until the calculated maximum accelerations matched the results of the calculations with the more complex multi-body model. The following span-dependent regression function for the additional damping ratio, hereafter referred to as $\Delta\zeta_{M2}$, for structures with spans up to 30 m (9) was subsequently derived to:

$$\Delta\zeta_{M2} = \frac{0,0187\,L - 0,00064\,L^2}{1 - 0,0441\,L - 0,0044\,L^2 + 0,000255\,L^3}, \text{ with } L \text{ [m]} \quad (9)$$

In the underlying calculations, negligibly slight deviations in the maximum structural acceleration with and without consideration of the VBI were computed for structures with spans exceeding 30 m, which is why the specifications in EN 1991–2:2003/AC:2010 [1] assume that the calculations with the moving load model for structures with larger spans are sufficiently accurate.

The assumptions on which these specifications are based comprise several inconsistencies and simplifications described in several studies [3,4,12]. As a result, calculations applying the additional damping according to [1] can, on the one hand, still yield very uneconomical results since the effects of the VBI cannot be taken into account sufficiently. On the other hand, in some applications, the accelerations comprising additional damping can result in excessive damping of the structures, thus yielding unsafe results compared to ones obtained with a more sophisticated interaction model.

2.3.3. M3 – Additional damping acc. to Yau et al. [10]

Yau et al. present in [10] an alternative analytical formulation of the additional damping that considers a larger number of bridge and vehicle parameters. The basis of the formulation is the comparison of a mechanical model of a train on the bridge structure (modeled as Bernoulli-Euler or Timoshenko beam) and an equivalent system of the bridge

structure without train but with an additional viscous damping ratio $\Delta\zeta$, which accounts for the damping contribution of interaction effects. From this, Yau et al. derive analytically an equation for the additional damping (schematically displayed in Fig. 3).

In the combined mechanical model, both the bridge structure and the vehicle are converted into an equivalent oscillator with a single degree of freedom (SDOF) according to their respective fundamental mode through modal analysis. Based on the assumption that there are always one front and one rear bogie of two adjacent coaches located on the bridge structure, the effective modal mass m_1, stiffness k_1, and damping coefficient c_1 of each half coach (one bogie, one half car body) can be calculated using the detailed interaction model as shown in Fig. 3 (modified from [10]). The equivalent SDOF oscillator of the bridge structure is based on the fundamental bending mode with its effective modal mass M_1, stiffness K_1, and damping coefficient C_1. Since the position of the two half coaches acting as passive vibration dampers on the equivalent system of the bridge structure is fixed in this approach (located symmetrically in the middle of the bridge), it is not possible to consider any time-depending effects due to the varying position of the train.

The damping contribution c_a of the vehicle (see Fig. 3 in far-right illustration) can be determined from the adjustment of the dynamic equivalence SDOF system of the bridge structure with the mass M_1, stiffness K_1, and damping coefficient $C_1 + c_a$ to the above-described multi-degree of freedom (MDOF) system concerning the vibration amplitude at resonance. Finally, this approach results in a formulation of the additional damping ratio $\Delta\zeta_{M3}$ by the following Eq. (10):

$$\Delta\zeta_{M3} = \mu_1 r_1 \sqrt{r_1^2 + \left(2\,\xi_1\right)^2} \quad (10)$$

with $\mu_1 = \dfrac{m_1}{M_1}; \quad \xi_1 = \dfrac{c_1}{2\,m_1\,\omega_1}; \quad r_1 = \dfrac{\omega_1}{\Omega_1}; \quad \omega_1 = \sqrt{\dfrac{k_1}{m_1}} \text{ and } \Omega_1 = \sqrt{\dfrac{K_1}{M_1}}$

$$(11)$$

The main influencing parameters in this equation are the ratio μ_1 of the modal mass of a half coach to the modal mass of the structure (only the first vibration modes), the ratio r_1 of the fundamental angular frequencies, and the Lehr's damping ratio ξ_1 of the modal equivalence system of the half coach.

2.3.4. M4 – Additional damping acc. to Stoura and Dimitrakopoulos [11]

Stoura and Dimitrakopoulos describe in [11] an analytical derivation of the additional damping, which the authors define based on the equations of motions for a bridge structure with arbitrary boundary conditions and a multi-body system of the crossing train. Both equations are subsequently coupled by assuming rigid and constant contact of wheelsets and the bridge structure, leading to an extended equation of
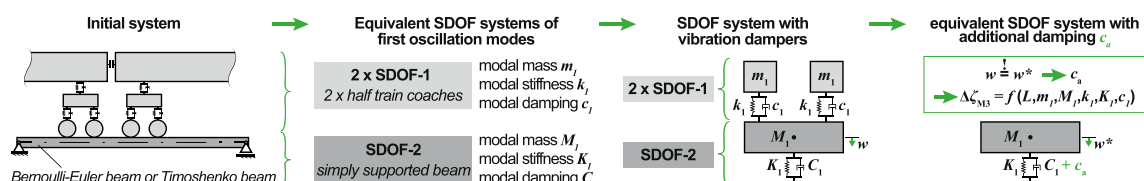
Fig. 3. M3 - schematic procedure of determination of additional damping acc. to [10].
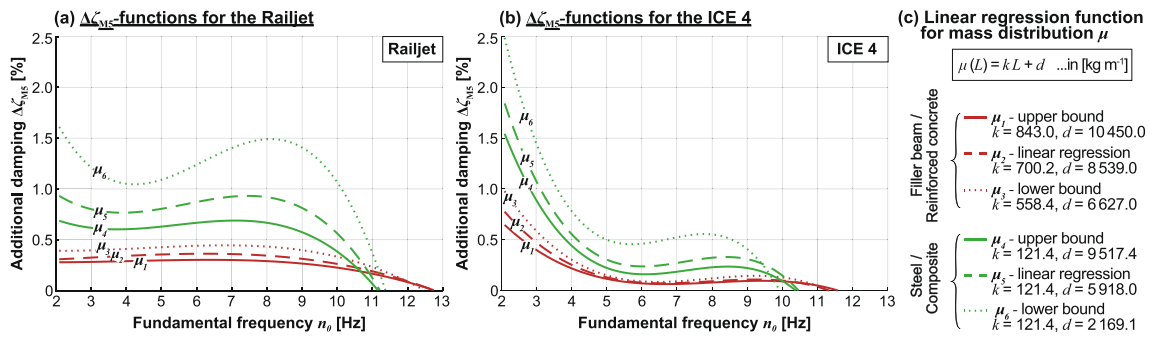
Fig. 4. M5 - additional damping functions acc. to [12] for two high-speed trains. (a) – Railjet; (b) – ICE 4.

motion for the bridge structure. The resulting notation enables the identification and further analysis of the time-dependent contributions due to VBI to the damping and stiffness matrix of the bridge structure and the vector containing the external loading. In addition, it allows to determine and evaluate the influence of controlling parameters on the damping contribution due to VBI, in other words, on the additional damping of the bridge.

Subsequently, the authors use simplified assumptions to define a time-independent formulation of the additional damping, which, according to numerical investigations, well conform with the results of calculations that take into account the time-dependent position change of the wheelsets on the bridge.

The additional time-independent damping for single-span girders, neglecting the wheelset masses, can be defined as modal damping ratios $\Delta\zeta_{i,M4}$ for each mode i and depends on the damping coefficient c_p of the primary suspension, the modal bridge mass M_i and angular eigenfrequency Ω_i of the bridge. Furthermore, the distance $\overline{d}$, which typically is not constant for every train coach, is included in Eq. (12). In the following investigations, $\overline{d}$ is determined in accordance with the approach of Stoura and Dimitrakopoulos [11] using the average distance between the maximum number n of axle loads which find place on the bridge (with span L) simultaneously acc. to Eq. (13).

$$\Delta\zeta_{i,M4} = \frac{c_p}{4\,M_i\,\Omega_i}\left(\frac{L}{i\,\overline{d}}+\frac{1}{2}\right) \tag{12}$$

with $\overline{d} = \dfrac{L}{n-1}$ (13)

For a better overview, the same symbols were used in Eq. (12), taken from [11] as by Yau et al. in [10].

2.3.5. M5 – Additional damping acc. to Glatz and Fink [12]

In [12], Glatz and Fink conduct extensive computational studies for four European high-speed trains (ICE 2, ICE 4, Eurostar, and Railjet) and a parameter field of bridge properties based on the characteristics of 210 single-span bridges.

The authors define span- and train-dependent regression functions for the lower and upper bound of fundamental frequencies n_0 and mass distribution μ of the bridges. With these functions, they specified 1080 different combinations of spans L, mass distributions μ, and fundamental frequencies n_0 for the calculations. The additional damping for each combination of bridge properties was determined by iteratively adapting the input parameters for MLM calculations until the results for the maximum acceleration in the predefined speed range met the results of reference calculations using the DIM.

Finally, a lower boundary function for the additional damping ratio $\Delta\zeta_{M5}$ (see Eq.(14)) is determined as a cubic polynomial function depending on the bridge's fundamental frequencies n_0, specified for each train and six different mass distributions (from μ_1 for heavy concrete structures to μ_6 for light steel structures).

$$\Delta\zeta_{M5}[\%] = a\,n_0^3 + b\,n_0^2 + c\,n_0 + d \tag{14}$$

The functions for either of the high-speed trains considered in this paper (Railjet and ICE 4) are plotted in Fig. 4 for masses from μ_1 to μ_6. The required function parameters for Eq. (14) are given in Table 1.

Glatz and Fink determine a strong dependency of the function course of $\Delta\zeta_{M5}$ on the considered train, while the mass distribution of the bridges primarily has a scaling effect (with $\Delta\zeta_{M5}$ increasing with decreasing mass distribution μ). Accordingly, the approach described in [12] can be applied only to the trains mentioned above, and bridge structures with properties within the examined parametric field of bridges (4 m $\leq L \leq$ 40 m, natural frequencies n_0 and mass distributions μ within regressions functions acc. to [12]). The structural damping ratio ζ in [12] was taken from the base values described in [1] and specified as follows:

$L < 20m \quad L \geq 20m$

Steel and composite bridges :
$$\begin{array}{l} L < 20\text{ m}: \ \zeta[\%] = 0.5 + 0.125\,(20-L) \\ L \geq 20\text{ m}: \ \zeta[\%] = 0.5 \end{array} \tag{15}$$

Filler beam and reinforced concrete bridges :
$$\begin{array}{l} L < 20\text{ m}: \ \zeta[\%] = 1.5 + 0.07\,(20-L) \\ L \geq 20\text{ m}: \ \zeta[\%] = 1.5 \end{array} \tag{16}$$

Furthermore, the authors encountered a substantial variation across results above a specific limit of fundamental frequencies for each of the considered train configurations and mass distributions. Consequently, they defined upper limits for the applicability of the derived regression functions.

The calculations in the present paper are based on linear interpolation of the resulting regression functions for $\Delta\zeta_{M5}$ for bridge structures with mass distributions in-between the defined functions for μ_1 to μ_6, following the recommendations in [12].

Table 1
Parameters for the lower bound function of additional damping acc. to [12].

		a	*b*	*c*	*d*
Railjet	μ_1	−5.631e-4	0.007015	−0.02098	0.2931
	μ_2	−5.083e-4	0.004266	0.006318	0.2768
	μ_3	−0.001104	0.01497	−0.05015	0.4376
	μ_4	−0.004615	0.07522	−0.3699	1.172
	μ_5	−0.007272	0.1238	−0.6329	1.78
	μ_6	−0.01547	0.2867	−1.598	3.844
ICE 4	μ_1	−0.003214	0.07749	−0.6049	1.604
	μ_2	−0.004115	0.09777	−0.7529	1.964
	μ_3	−0.005526	0.1301	−0.9886	2.531
	μ_4	−0.01156	0.252	−1.783	4.283
	μ_5	−0.01389	0.3006	−2.11	5.076
	μ_6	−0.02314	0.4684	−3.087	7.118

Table 2
Train parameters for the MLM and the DIM of the Railjet and ICE 4.

Train type		Railjet [26]		ICE 4 [30]	
car order		[Loc - 7 × PC] - [7 × PC - Loc] →		[UPC - 2 × PPC - UPC - 2 × PPC - UPC - PPC - UPC - PPC - 2 × UPC] →	
		Loc	PC	PPC	UPC
F_{stat}	[kN]	215.6	148.4	174.2	161.4
m_c	[kg]	51 500	47 316	52 896	55 279
I_c	[kg m]	882e3	307e4	355e4	391e4
m_b	[kg]	13 220	2 800	4 427	2 414
I_b	[kg m]	27 100	1 700	3 090	770
m_w	[kg]	2 495	1 900	2 322	1 430
d	[m]	18.59	26.50	28.75	28.75
r	[m]	9.90	19.00	19.50	19.50
b	[m]	3.00	2.50	2.60	2.30
k_p	[kN m^{-1}]	3 680	1 690	2 000	13 000
c_p	[kN s m^{-1}]	80	20	20	0
k_s	[kN m^{-1}]	2 720	280	5 000	720
c_s	[kN s m^{-1}]	200	14	20	10
n_p	[Hz]	3.76	5.53	4.78	16.52

3. Scope of the numerical investigations

In order to evaluate the effect of considering the influence of VBI according to the five mentioned approaches M1 to M5, calculations are performed for two different high-speed trains and 65 bridge structures.

3.1. Vehicle properties

The two considered high-speed trains are the Railjet and the ICE 4. The Railjet is a conventional train with fourteen passenger cars (PC) and two locomotives (Loc), one at each end of the train. The ICE 4 is a multiple-unit train with partly powered axles. In the following, a twelve-part train consisting of six powered passenger cars (PPC) and six unpowered passenger cars (UPC) will be investigated. All calculations described in the following sections were carried out with the MLM and the DIM of both trains. The required vehicle parameters (compiled in Table 2) were taken from [26,30].

The natural frequency n_p for vertical vibrations of the primary suspension stage can be approximated according to [8] by applying Eq. (17), whereby the bogie mass supported by two springs is assumed isolated from the rest of the vehicle.

$$n_p = \frac{1}{2\pi}\sqrt{\frac{2\,k_p}{m_b}} \tag{17}$$

Calculations were also performed with the MLM and the five different approaches for considering VBI effects, which are subsequently referred to with the indices M1 (ÖBB guidelines [9]), M2 (EN 1991–2:2003/AC:2010 [1]), M3 (Yau et al. [10]), M4 (whereby modal damping ratios $\Delta\zeta_{M4,i}$ were applied acc. to Stoura and Dimitrakopoulos [11]), and M5 (Glatz and Fink [12]).

The modal vehicle parameters of the Railjet, required for the calculation of the additional damping acc. to M3 [10] and M4 [11], are based on the data of the passenger cars (see Table 2). Since there are also significant differences in the properties of the powered and unpowered passenger cars of the ICE 4 – especially regarding the damping properties of the primary stage – the additional damping acc. to M3 was determined for both car types. For the application of M4, the specification of a primary damping coefficient c_p is essential (see Eq. (12)). Since in [30] c_p is assumed to be zero for the unpowered car, M4 can only be applied to the powered cars.

3.2. Structural properties

The properties of the 65 considered bridge structures were taken from a catalog of existing single-span bridges in Austria, subdivided into 17 steel or composite structures and 48 reinforced concrete or filler beam structures. Their characteristics L, n_0, μ and ζ and the linear regression functions for μ_1 to μ_6 as defined in [12] are represented graphically in Fig. 5. Additionally, the combinations of properties used for the calculations in [29] (forming the basis of the current standard specifications M2 acc. to [1]) are plotted as black squares in Fig. 5.

The structural damping ratios ζ of 26 of the 65 bridges were determined experimentally through in-situ measurements. The damping ratios of the other bridges were calculated using the span-dependent lower bound functions for ζ specified in [1] for different bridge types (illustrated in Fig. 5–c).
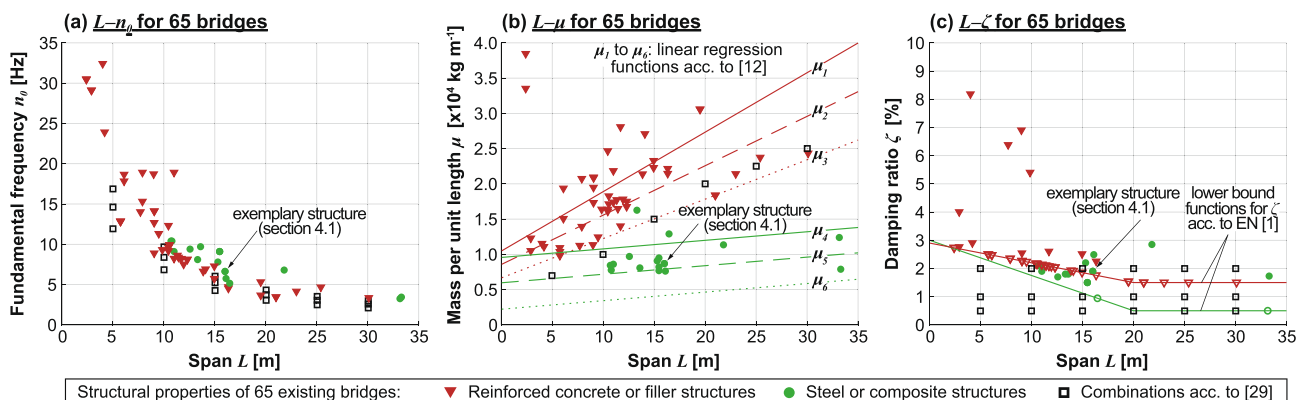
Fig. 5. Structural properties of 65 bridges for numerical analysis. (a) – span/fundamental frequency; (b) – span/mass per unit length; (c) – span/damping ratio.
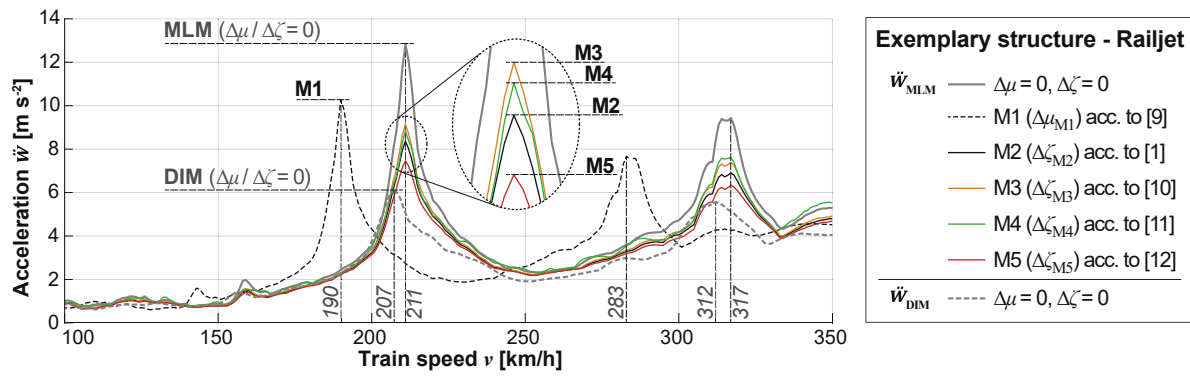
Fig. 6. Maximum acceleration over train speed - comparative calculations for one exemplary bridge.

4. Evaluation of results

Comparative calculations with either load models DIM and MLM are performed to evaluate the success of considering the vibration-damping effects of VBI in calculations with the simplified MLM by applying one of those methods. Seven different calculations were performed for each bridge: one reference calculation with the DIM, one MLM calculation without any additional mass or damping, and five MLM calculations applying one of the approaches M1 to M5.

The bridge vibrations are numerically calculated considering three bridge vibration modes in Eq. (4) and a speed range of the trains between 100 and 350 km/h, discretized in 1 km/h steps.

The maximum accelerations $\ddot{w}_{MLM}$ at the midspan of the bridge in the considered range of speeds calculated with the MLM with and without additional mass or damping are compared to the more realistic and usually smaller accelerations $\ddot{w}_{DIM}$ obtained with the DIM. The relative deviation $\delta\ddot{w}$ acc. to Eq. (18) is used as a comparative value. Likewise, the deviation of the train speed δv at which the maximum acceleration peaks of different calculations occur can be determined.

$$\delta\ddot{w}[\%] = 100 \frac{\ddot{w}_{MLM} - \ddot{w}_{DIM}}{\ddot{w}_{DIM}},$$
$$\delta v[\%] = 100 \frac{v_{MLM} - v_{DIM}}{v_{DIM}} \tag{18}$$

The vertical deformations w could be compared according to the same principle. The following evaluations focus on the accelerations since the calculations yield deformations w_{MLM} above the normative limit of $L/600$ acc. to [7] in very few of the 65 investigated structures (ICE 4: 0 bridges, Railjet: 3 bridges), whereas the accelerations $\ddot{w}_{MLM}$ exceed the normative limit of $\ddot{w} \leq 3.5$ m/s² in a considerable number of cases (for both trains: 46 bridges) in the investigated speed range. It should be noted that the following findings regarding the effects of applying M1 to M5 generally also apply to the calculation results of vertical deformations. For more clarity, these evaluations were not included in this article.

This evaluation focused on the acceleration peaks due to resonance, which generally represent the maximum acceleration values within the considered speed range. Only local maximum values were considered in the evaluations according to Eq. (18). Resonance peaks occur mainly at train speeds in proximity to $v_{crit,i,j}$, the critical speeds at which the regularly spaced train axles exert a periodic excitation with a frequency $n_j = j\, v_{crit,i,j}/d$ corresponding to the fundamental frequency $n_{0,i}$ of the bridges:

$$v_{crit,i,j} = \frac{n_{0,i}\, d}{j}, \quad i = 1, 2, \cdots; \ j = 1, 2, \cdots \tag{19}$$

Peak values of accelerations in calculations using the DIM tend to occur at lower crossing speeds than those using the MLM. This is explained by the decrease of the fundamental frequencies of the bridges due to the consideration of the unsprung wheelset masses and other VBI

effects, which leads to resonance vibrations at lower train speeds. Only local maxima of accelerations at similar train speeds are included in the following evaluations. Thus, just peak accelerations corresponding to the same resonance situation are compared.

In the case of MLM calculations applying one of the five additional mass/damping approaches, positive values of $\delta\ddot{w}$ generally correspond to results on the safe side since the results from MLM calculations tend to overestimate the more realistic calculation results from the DIM. Therefore, positive values of $\delta\ddot{w}$ are explicable with insufficient additional damping or mass. The smaller the positive values $\delta\ddot{w}$, the better is the desired approximation of the acceleration results of calculations with the different vehicle models. Also, in the few cases in which the acceleration results obtained with the DIM exceed the results obtained with the MLM, positive values of $\delta\ddot{w}$ correspond to results on the safe side since they imply higher acceleration results in calculations with the MLM and additional mass/damping than in calculations with the DIM. Negative results characterize a non-conservative reduction in the maximum acceleration due to the additional mass or damping.

4.1. Exemplary structure

The calculation results of all seven calculation variants (Railjet: MLM with and without additional mass/damping, DIM) for one exemplary bridge are displayed in Fig. 6. The structural parameters of the bridge, summarized in Table 3 and highlighted in Fig. 5 ("exemplary structure"), correspond to the properties of an existing steel structure for which the fundamental frequency n_0 and Lehr's damping ratio ζ were determined experimentally. The mass per unit length μ of this bridge structure lies slightly above the linear regression function $\mu_5 [\mathrm{kgm^{-1}}] = 121.4\, L + 5918$ for steel and composite bridges (see Fig. 5).

The additional parameters required for applying M3 (Eq. (10)) and M4 (Eq. (12)) are given in Table 4. The modal vehicle parameters of the Railjet, necessary for the calculation of the additional damping ratios $\Delta\zeta_{M3}$ and $\Delta\zeta_{M4,i}$ acc. to [10 and 11] are based on the information of the passenger cars (see Table 2).

The bold gray line with the highest acceleration peak in Fig. 6 corresponds to the calculation results obtained with the MLM and no additional mass or damping of the bridge structure. The highest acceleration peak occurs at $v = 211$ km/h, which represents the resonance speed at which the fundamental mode of vibration is being exerted in every third oscillation period ($v_{crit,1,3}[\mathrm{km/h}] = 3.6 \frac{n_0\, d}{3}$, with $d = 26.5$ m).

Table 3
Exemplary bridge: structural parameters.

L [m]	μ [kg m⁻¹]	EA_{zz} [kN m²]	n_0 [Hz]	$\zeta_{meas.}$ [%]
16	8 690	10.1e3	6.63	1.9

Table 4

Input parameters for calculating the additional damping.

	Modal bridge parameters						Modal vehicle parameters			
	Ω_i [rad s^{-1}]			M_i [kg]	K_i [kN m^{-1}]			ω_1 [rad s^{-1}]	m_1 [kg]	c_1 [kN s m^{-1}]	$\bar{d}$ [m]
$i=1$	$i=2$	$i=3$		$i=1$	$i=2$	$i=3$				
41.56	166.25	374.07	69 520	120e3	192e4	973e4	3.3049	24 074	12.367	5.333

A second acceleration peak can be observed at $v_{\mathrm{crit,1,2}} = 317$ km/h.

The lowest gray dashed line illustrates the results of the DIM calculation. As mentioned before, the maximum acceleration peaks occur at lower critical speeds $v = 207$ km/h and $v = 312$ km/h, respectively, due to the additional train masses, the contribution of which is considered in the DIM calculations implicitly.

The calculation results obtained from the MLM with additional mass or damping acc. to the five methods are displayed with thin lines.

The additional mass $\Delta\mu_{\mathrm{M1}} = 2\,000$ kg m^{-1} applied acc. to M1 [9] significantly reduces the local acceleration maximum. In addition, increasing the structural mass leads, as described in [9], to a decrease in the natural frequency of the bridge and thus the critical speed v at which the acceleration maximum occurs to $v = 190$ km/h ($\delta v = $ -8.21 %). Also, the train speed at which second highest peak occurs is reduced to $v = 283$ km/h ($\delta v = $ -10.73 %). In the case of the exemplary structure, however, increasing the structural mass does not result in any additional acceleration peaks in the high-speed range that would not be recorded by DIM calculations. For such cases, the ÖBB guidelines [9] prescribe that these additional acceleration peaks must also be used to verify compliance with normative limits.

It can be observed that the consideration of additional damping ratios $\Delta\zeta_{\mathrm{M2}}$ to $\Delta\zeta_{\mathrm{M5}}$ in MLM calculations exerts only a scaling influence on the results and leads to significantly decreased maximum structural accelerations compared to calculations without additional damping. The respective peak accelerations still exceed the results obtained with the

DIM by at least $\delta\ddot{w} = 23.1$ %, i. e., on the safe side. The numerically derived additional damping ratio $\Delta\zeta_{\mathrm{M5}}$ acc. to [12] features the highest value of $\delta\ddot{w}$. Thus, in the case of this exemplary bridge, its consideration leads to results closest to the ones obtained with the DIM calculations. The calculation results taking into account $\Delta\zeta_{\mathrm{M3}}$ acc. to [10] and $\Delta\zeta_{\mathrm{M4}}$ acc. to [11] are very close to each other, but both exceed the results obtained with the normatively specified additional damping ratio $\Delta\zeta_{\mathrm{M2}}$ acc. to [1].

The values $\Delta\mu$ or $\Delta\zeta$ of each calculation method (in the case of the method acc. to [11], the modal values $\Delta\zeta_{\mathrm{M4},i}$) and the obtained maximum bridge accelerations $\ddot{w}_{max}$ are compiled in Table 5. Additionally, the resulting relative deviations $\delta\ddot{w}$ and δv for each calculation variant but only the maximum acceleration peak are given.

4.2. Numerical study

Following the same procedure described in section 4.1, the 65 bridge structures were examined with vehicle models of both trains (Railjet and ICE 4) and applying the five additional mass or damping methods, and the results of the maximum accelerations were compared to each other. As observable in Fig. 6 at $v = 317$ km/h, lower acceleration maxima will not be considered in the following evaluations since only the largest acceleration maximum of each bridge is taken into account. An overview regarding the reduction potential by considering the effects of VBI is given in Fig. 7.

Table 5

Additional mass/damping and calculation results for exemplary structure.

	DIM	MLM	M1 [9]	M2 [1]	M3 [10]	M4 ($\Delta\zeta_{\mathrm{M4}i}$) [11]		M5 [12]
$\Delta\mu$ [kg m^{-1}] or $\Delta\zeta$ [%]	–	–	2 000 kg m^{-1}	0.637 %	0.481 %	$i = 1$	0.606 %	0.854 %
						$i = 2$	0.087 %	
						$i = 3$	0.030 %	
$\ddot{w}_{\mathrm{max}}$ [m s^{-2}]	6.06	12.80	10.27	8.36	9.16	8.85		7.46
$\delta\ddot{w}$ [%]	∓ 0	+111.22	+69.47	+37.95	+51.16	+46.04		+23.10
δv [%]	∓ 0	+1.93	−8.21	+1.93	+1.93	+1.93		+1.93
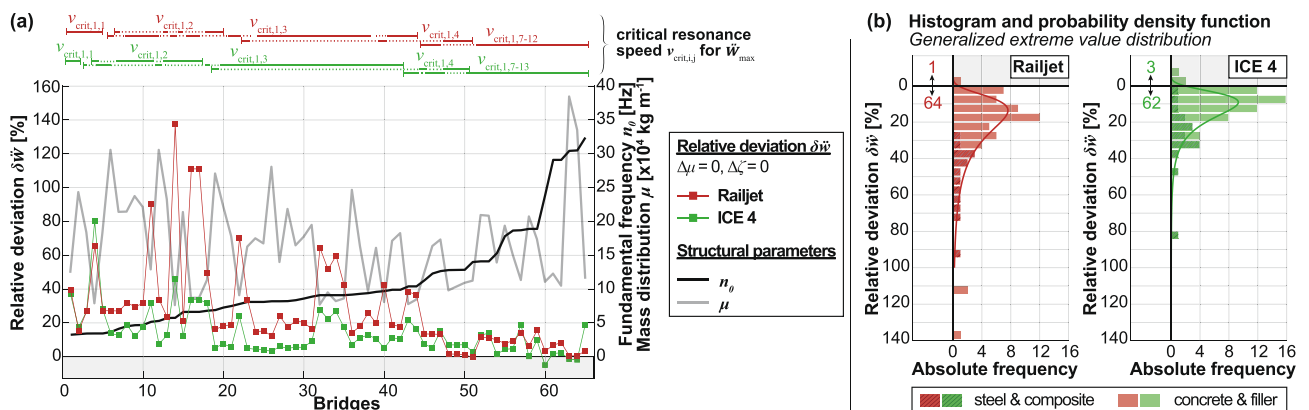
Fig. 7. Relative deviations of accelerations for 65 bridge structures (MLM compared to DIM). (a) – results sorted by structure's fundamental frequency; (b) – histogram and fitted probability density function of results.
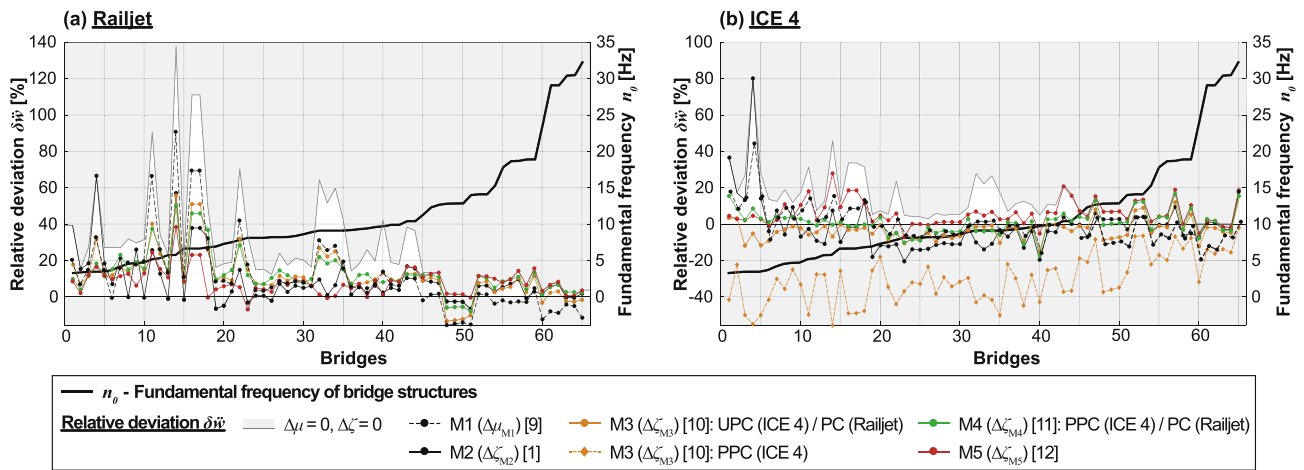
Fig. 8. Relative deviation of acceleration results from five approaches for consideration of VBI. (a) – results for the Railjet; (b) – results for the ICE 4.

Fig. 7-a shows graphically the resulting values of $\delta\ddot{w}$ which is the relative deviations of the maximum accelerations from MLM calculations (without additional mass or damping) compared to the reference values of the DIM calculations. The results are generally plotted as markers, while the connecting lines are only for further visualization, whereby the results obtained with the Railjet are displayed in red, those obtained with the ICE 4 in green color. The bridges are sorted by their fundamental frequencies n_0 visualized by the bold black line corresponding to the right ordinate (3.25 Hz $\leq n_0 \leq 32.4$ Hz). The bold gray line visualizes the mass distribution μ ($7\,620$ kg m^{-1} $\leq \mu \leq 38\,450$ kg m^{-1}) of each bridge.

Fig. 7-b shows the histogram and a fitted probability density function of the resulting $\delta\ddot{w}$ for both train types, whereas calculations performed with the vehicle model of the Railjet lead to results with a broader spread and for a larger number of bridge structures (64) to values of $\delta\ddot{w}$ significantly above zero. The contrast of shading of the histogram distinguishes the bridge types. It should be noted that, for both trains, the highest results of $\delta\ddot{w}$ and, therefore, the most significant potential for vibration-reducing impact of VBI is in the steel and composite structures.

The consideration of VBI by applying the DIM usually leads to decreased structural vibrations, which is reflected in the results of $\delta\ddot{w}$ for both train types, represented by the red and the green markers in Fig. 7-a that take negative values only in four cases (three for the ICE 4, for the Railjet). Generally, it can be observed that, especially for bridges with $n_0 \lesssim 12$ Hz, there is a significant potential to reduce the acceleration maxima by considering VBI, as the MLM results without additional damping take values up to 138 %. Furthermore, the most significant reduction of maximum accelerations due to consideration of VBI effects can be observed in bridges with a low mass distribution μ. This corresponds to the findings in [12] that a particularly strong influence of the VBI is to be expected for low bridge masses and similarity of the natural frequency of the bridge n_0 and the primary suspension stage n_p

according to equation (17), which is for both trains (except for the unpowered passenger cars of the ICE 4) below 6 Hz. In this regard, the bridge mass seems to be of greater importance.

With increasing fundamental frequencies of the considered bridge structures, the maximum acceleration peaks occur at high-order resonance events $v_{\mathrm{crit},i,j}$. Concurrently, high fundamental frequencies are associated with a lower influence of the vehicle-bridge-interaction and thus with a lower relative deviation $\delta\ddot{w}$ of the maximum acceleration results of both train models MLM and DIM.

Fig. 8 illustrates the values of $\delta\ddot{w}$ based on the maximum acceleration results from MLM calculations – in contrast to the previous evaluations displayed in Fig. 7 with additional mass or damping – compared to maximum accelerations of the corresponding DIM calculations for the considered 65 bridges and the Railjet (Fig. 8-a) and ICE 4 (Fig. 8-b). The results of $\delta\ddot{w}$ obtained without considering additional mass or damping in the underlying MLM calculation results (displayed in Fig. 7-a by the red and green markers) can be considered as upper bounds for results with consideration of vehicle-bridge-interaction and are in Fig. 8 represented by the upper limitations of the white areas. The lower bound is formed by $\delta\ddot{w} = 0$ % since, as mentioned above, negative values of $\delta\ddot{w}$ indicate excessive additional damping by the considered approach and unsafe results.

In most cases, the implementation of an additional damping ratio $\Delta\zeta$ yields results closer to the ones obtained with the DIM, but a large number of negative and, therefore, non-conservative values of $\delta\ddot{w}$ is apparent, especially in the case of the ICE 4. Implementing an additional mass $\Delta\mu$ acc. to [9] shifts for the ICE 4, in two cases, the critical speed v at which the maximum acceleration occurs below 100 km/h. These two bridges are excluded from the following evaluations.

In Table 6, the minimum, maximum, arithmetic mean results and standard deviation σ of $\delta\ddot{w}$ as well as the number of negative (unsafe) results for each method of determination of $\Delta\mu$ or $\Delta\zeta$ are compiled. The

Table 6

Characteristic results of $\delta\ddot{w}$ for 65 bridge structures and five approaches for vehicle-bridge-interaction.

Train		Railjet					ICE 4				
		$\delta\ddot{w}$ [%]				No. of $\delta\ddot{w} < 0$ %	$\delta\ddot{w}$ [%]				No. of $\delta\ddot{w} < 0$ %
		Min	Max	Mean	σ		Min	Max	Mean	σ	
$\Delta\mu=\Delta\zeta=0$ %		−0.40	137.86	27.77	27.59	1	−5.01	80.21	13.77	13.44	3
M1 [9]		−15.73	90.77	11.02	20.40	17	−19.52	44.37	−0.56	9.95	37
M2 [1]		−6.57	66.60	9.28	14.10	15	−20.34	80.21	−1.29	14.28	44
M3	**PC/PPC**	−13.34	55.77	11.98	13.37	8	−55.29	−2.08	−30.13	13.09	65
[10]	**UPC**	/	/	/	/	/	−14.54	13.94	−3.19	5.53	57
M4 [11]		−7.85	50.14	12.81	11.23	4	−17.30	16.75	0.90	6.40	28
M5 [12]		−6.89	38.40	8.37	7.14	5	−6.98	27.97	6.02	6.80	7
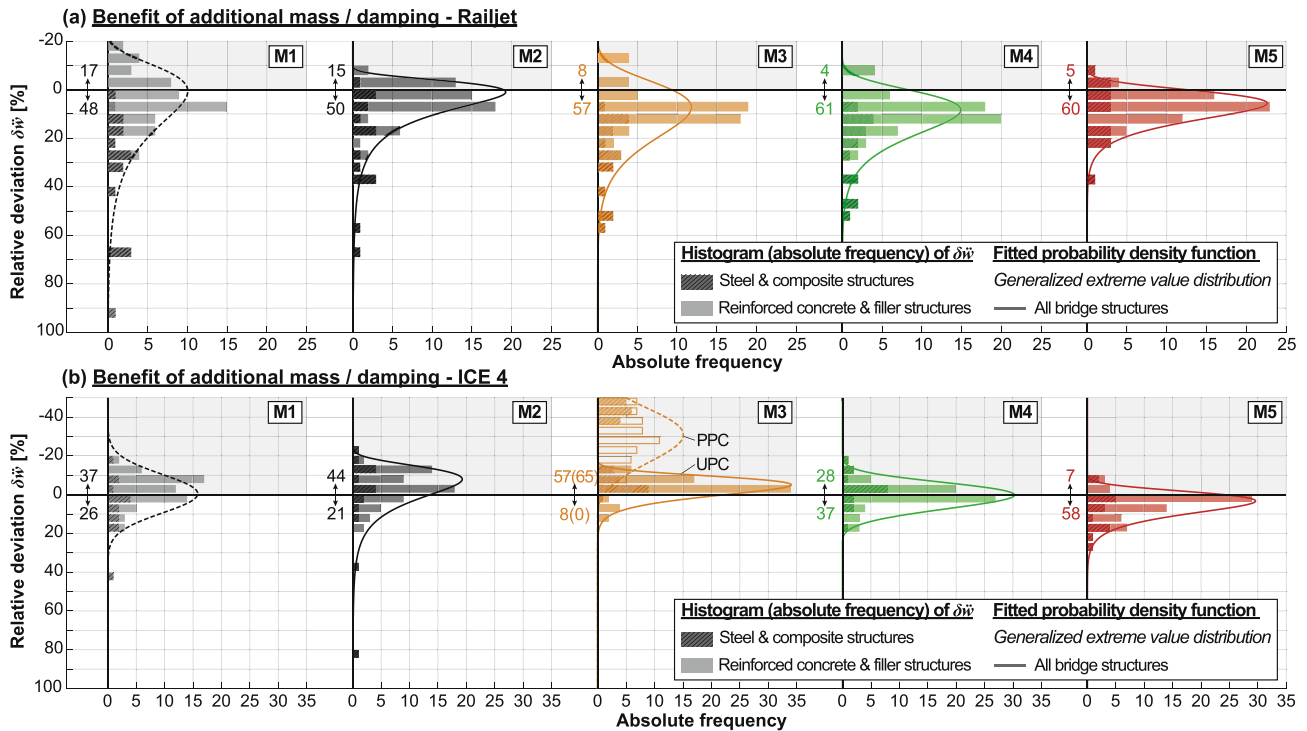
Fig. 9. Evaluation of histograms and fitted probability density functions of $\delta\ddot{w}$. (a) – Railjet; (b) – ICE 4.

best and worst results (best results defined as closest to the DIM results with a minimum number of negative results) in each category are marked with green or red shading respectively (excluding the results obtained with $\Delta\mu = \Delta\zeta = 0$). Further, the evaluation of the histograms and probability density functions (assuming generalized extreme value distribution) is graphically displayed in Fig. 9.

The normatively specified approach acc. to [1] yields negative and, therefore, unsafe values of $\delta\ddot{w}$ in 15 of 65 cases (for the Railjet) and in 44 of 65 cases (for the ICE 4). Applying an additional mass acc. to the ÖBB guidelines [9] to Railjet calculations causes an increase in the mean and maximum values $\delta\ddot{w}$ compared to the standard [1], and also a higher number of unsafe results (17 out of 65). In the case of the ICE 4, the approach of the ÖBB guidelines performs slightly better than the standard specifications [1], but it is still associated with a high number of negative values of $\delta\ddot{w}$ and therefore, in individual cases, a substantial overestimation of the damping effects of vehicle-bridge-interaction.

In the case of the ICE 4, the consideration of additional damping acc. to Yau [10] also appears to overestimate the damping effect strongly. If applied based on the characteristics of the powered car (PPC - yellow diamonds in Fig. 8-b), all results are significantly on the unsafe side, and for unpowered cars (UPC - yellow circles) in 57 of 65 cases.

For calculations with the Railjet, the results obtained by applying $\Delta\zeta_{M5}$ acc. to [12] yield, on average, the results closest to those obtained with the DIM. The approaches described in [10] (only applied to the passenger car PC) and [11] yield, on average, worse results than the normatively specified approach in [1] but still produce lower maximum values of $\delta\ddot{w}$ than the normative approach, and very few negative results. For the ICE 4, both the approaches acc. to [11] (green markers) and [12] (red markers) are capable of reflecting the influence of vehicle-bridge-interaction quite well, with the approach in [12] yielding fewer non-conservative results and the approach in [11] resulting in the lowest average deviation of <1 %.

Fig. 9 again visualizes the substantial underestimation of damping effects due to vehicle-bridge-interaction by applying additional mass $\Delta\mu$ acc. to the ÖBB guidelines [9] or additional damping $\Delta\zeta_{M2}$ acc. to the normative recommendations [1] in calculations performed for the

Railjet, as well as the overestimation in the case of the ICE 4 leading to a high number of unsafe results. Especially both recently developed methods M4 and M5 for determining the additional damping ratio acc. to [11,12] perform better, which is apparent in the lower spread of results and shift towards positive values of $\delta\ddot{w}$.

The contrast of shading of the histogram distinguishing between steel and concrete structures shows, especially with method M5 for both trains, a relatively similar distribution of the results, while M1, M3, and M4 in the case of the Railjet yield high values of $\delta\ddot{w}$ in steel and composite structures.

4.3. Influence of structural parameters

This section deals with the question of whether the deviation $\delta\ddot{w}$ of the maximum acceleration values obtained by applying one of the five methods for consideration of VBI in MLM calculations, in comparison to applying the more accurate DIM, is dependent on any structural parameters. To distinguish between the different methods, the notation $\delta\ddot{w}_{MLM}$ for results of $\delta\ddot{w}$ obtained without additional damping or mass, and $\delta\ddot{w}_{Mj}$ for results of $\delta\ddot{w}$ obtained by applying method Mj (j = 1, 2, …, 5) will be used in the following evaluations. Both $\delta\ddot{w}_{MLM}$ and $\delta\ddot{w}_{Mj}$ use the acceleration maxima from calculations with the DIM as the reference value, as specified in Eq. (18).

In order to visualize potential dependencies, it is helpful to plot the results of $\delta\ddot{w}_{Mj}$ against structural parameters coming into question as explanatory variables and to fit a regression model to the results. The aim is to find a simple linear regression model with only one independent variable x and a preferably high significance. The linear regression models for each method, M1 to M5, take the form

$$\delta\ddot{w}_{Mj,i} = \alpha + \beta x_i + \varepsilon_i, \quad j = 1, 2, \cdots, 5; \quad i = 1, 2, \cdots \quad (20)$$

with x_i being the explanatory variable and ε_i the error of each observation. The coefficients α and β were estimated with ordinary least squares without weighting (for instance, described in [31]).

First, the relation between the general effect of considering VBI by applying a multi-body vehicle model (DIM) and the effect of applying
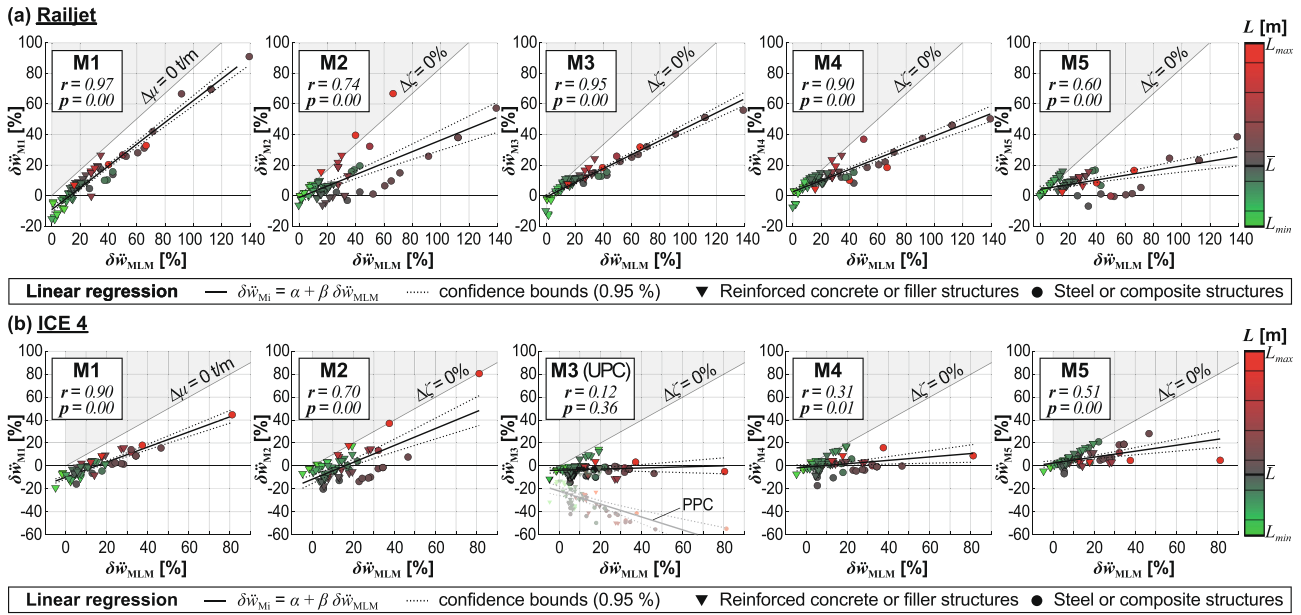
Fig. 10. Relation between the effect of applying M1 to M5 ($\delta\ddot{w}_{\text{Mj}}$) and general VBI effects on maximum bridge acceleration ($\delta\ddot{w}_{\text{MLM}}$). (a) – Railet; (b) – ICE 4.

one of the alternative methods, M1 to M5, is evaluated. Fig. 10 shows in each subdiagram the resulting relative deviations $\delta\ddot{w}_{\text{Mj}}$ calculated with method Mj against the respective deviations $\delta\ddot{w}_{\text{MLM}}$ of each bridge on the abscissa, characterizing the vibration damping benefit of applying the DIM. Furthermore, the bridge type is identified using different marker types, whereby again, reinforced concrete and filler structures are marked with triangles and steel and composite structures with circles.

The respective span L of each bridge is given on a color scale, which takes on a gray shade at the average span of $\overline{L} = 12.77$ m, and displays larger spans with red and smaller spans with green color. The gray areas in the top left represent the upper boundary of results $\delta\ddot{w}_{\text{Mj}}$, i. e., the acceleration results obtained by applying M1 to M5 equal or exceed the results obtained without additional mass or damping ($\Delta\mu = \Delta\zeta = 0$).

Finally, linear regression functions of the form given in Eq. (20) are fitted to the results of $\delta\ddot{w}_{\text{Mj}}$, whereby $\delta\ddot{w}_{\text{MLM}}$ is used as an explanatory variable. Fig. 10 graphically shows the estimated regression functions and 95 % confidence intervals. The results of M3 applied for the powered passenger cars of the ICE 4 are plotted with low opacity and are disregarded in the following evaluations. The correlation coefficients r and the p-value (p) for each regression function are noted in the subfigures, and their definition can be found, amongst others, in [31]. The Pearson correlation factor r reflects the degree of linear relation between the results of $\delta\ddot{w}_{\text{Mj}}$ and $\delta\ddot{w}_{\text{MLM}}$, while the p-value gives the probability of the assumed null hypothesis being true, which is, in this case, no relationship of $\delta\ddot{w}_{\text{Mj}}$ and $\delta\ddot{w}_{\text{MLM}}$. Therefore, high values of p would require the rejection of the linear correlation model while low values (usually $p \leq 0.05$) indicate a high significance of the chosen correlation model.

From the subfigures in Fig. 10-a and b corresponding to M1, it can be observed that there is a strong positive correlation between the vibration-damping impact of applying the method and utilizing the more complex DIM. This indicates that M1 can generally reproduce the impact of the VBI less well as the influence of the VBI increases. With a modest influence of the VBI on the maximum accelerations ($\delta\ddot{w}_{\text{MLM}} < 20$ %), applying M1 often results in negative results.

This tendency is also given in the results of the other four methods, but the correlation factors between $\delta\ddot{w}_{\text{MLM}}$ and $\delta\ddot{w}_{\text{Mj}}$ is generally lower, especially in the case of the ICE 4. In particular, when M3 is applied to the unpowered and M4 to the powered passenger cars, the correlation

factors are very low.

It can be observed in both trains that a significant underestimation of the damping effect occurs for structures with a particularly small or large span. This indicates that the span-dependent determination function acc. to Eq. (9) [1] reflects the damping effect of VBI in its edges insufficiently.

In order to determine the relation between $\delta\ddot{w}_{\text{Mj}}$ and the bridge's structural parameters, linear regression models with one explanatory variable as described in Eq. (20) were fitted to the results of $\delta\ddot{w}_{\text{Mj}}$ with different structural properties as the independent variable x_i. The four structural parameters span L, mass per unit length μ, fundamental frequency n_0 and structural damping ratio ζ, as well as their linear, quadratic, and rational combinations, were considered explanatory variables.

In order to keep the regression model as simple as possible, only one linear term, i.e., only one possible explanatory variable, was taken into account. With this restriction, regression models with $x_i = L/\mu$ as the explanatory variable result in high significance for all methods, recognizable by low p–values ≤ 0.05.

This evaluation is displayed in Fig. 11. Again, the respective values of $\delta\ddot{w}_{\text{Mj}}$ obtained with each method are plotted in the subfigures, but now against the spans L of the bridges. The color scale characterizes the mass distribution of the bridges, with gray markers indicating an average mass distribution $\overline{\mu}$, and again green and red markers indicating lower respective higher values of μ. In each subfigure for one method and train, the resulting linear regression functions $x_i = L/\mu$ were evaluated and plotted for three constant-held mass distributions: for $\mu_{min} = 7\,620$ kg m^{-1} (green dashed line), for $\mu_{max} = 38\,440$ kg m^{-1} (red dashed line) and for the average mass distribution $\overline{\mu} = 16\,540$ kg m^{-1}. Therefore, possible interaction effects of span L and mass distribution μ can be observed in Fig. 11. The annotated correlation coefficients r and p-values refer to the correlation of $\delta\ddot{w}_{\text{Mj}}$ and L/μ.

All methods (except for M3 for the ICE 4) display a positive correlation of span L and relative deviation $\delta\ddot{w}_{\text{Mj}}$, whereby M5 in the case of the Railjet and M3 to M5 in the case of Railjet feature an almost constant slope. The p-values of M3 and M4 in the case of the ICE 4 indicate no statistical significance and suggest evidence for the null hypothesis (no linear relation of $\delta\ddot{w}_{\text{Mj}}$ and L/μ).

Bridges with a low mass distribution μ yield in the case of the Railjet and especially at medium spans L the highest values of $\delta\ddot{w}_{\text{Mj}}$, i.e.,
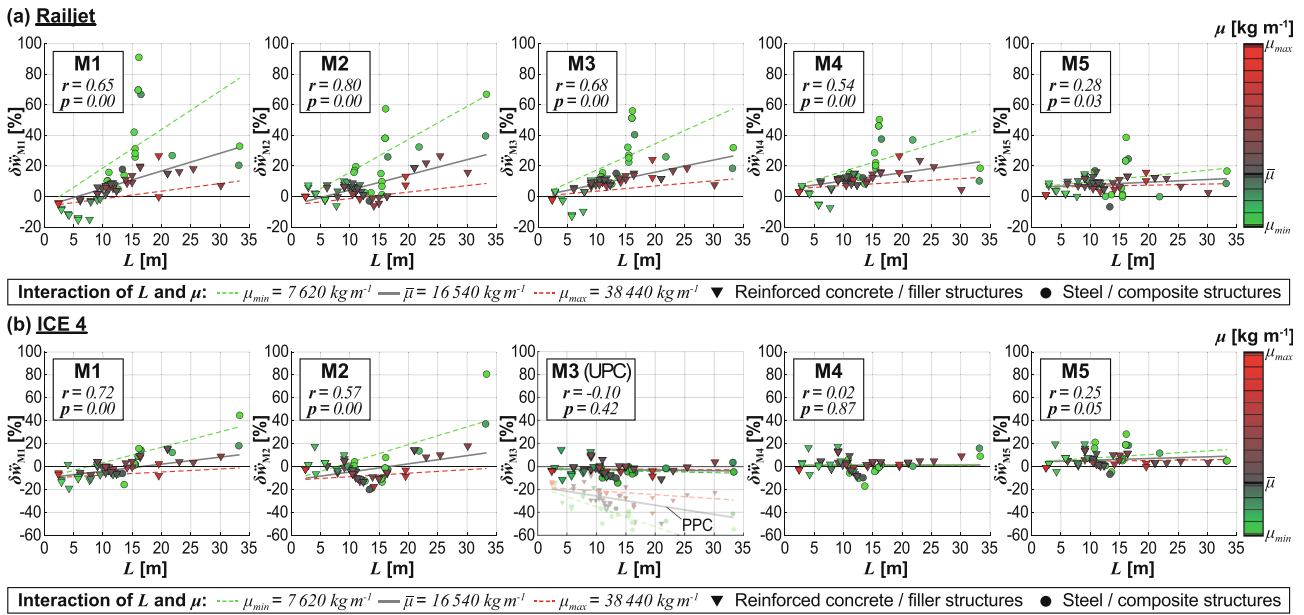
Fig. 11. Relation between the effect of applying M1 to M5 ($\delta\ddot{w}_{Mj}$) and L/μ. (a) – Railet; (b) – ICE 4.
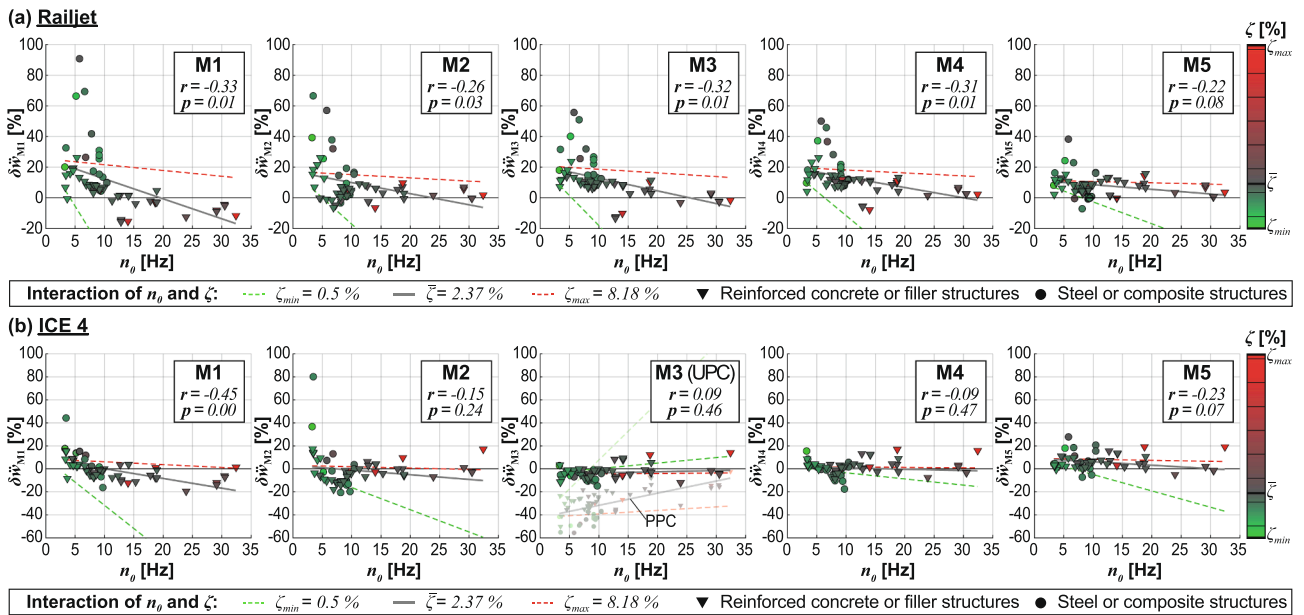
Fig. 12. Relation between the effect of applying M1 to M5 ($\delta\ddot{w}_{Mj}$) and n_0/ζ. (a) – Railet; (b) – ICE 4.

insufficient allowance for VBI effects with the alternative consideration methods. Also, in the case of the ICE 4, these bridges tend to result in the highest and lowest values of relative deviation $\delta\ddot{w}_{Mj}$.

Following the same principle as in Fig. 11, Fig. 12 shows the correlation of $\delta\ddot{w}_{Mj}$ and n_0/ζ and potential interaction effects of the fundamental frequency n_0 and damping value ζ of the bridges. All 65 bridges were included in this evaluation, regardless of whether the structural damping value was determined experimentally or by applying the lower bound functions acc. to [1]. Statistically significant correlations were only determined for M1 to M4 in the case of the Railjet and M1 in the case of the ICE 4.

As shown in Fig. 8, it can be observed from Fig. 12 that the highest deviations $\delta\ddot{w}_{Mj}$ occur for bridges with a fundamental frequency $n_0 \lesssim 12$ Hz, while negative values mainly occur for bridges with higher fundamental frequencies, except for the results of $\delta\ddot{w}_{M3}$ in the case of the ICE

4. In this regard, M2 acc. to [1] yields for bridges with a similar fundamental frequency, especially in the case of the ICE 4, very high as well as negative values of $\delta\ddot{w}_{Mj}$, indicating additional interaction effects due to the length L and mass distribution μ as shown in Fig. 11. There is no apparent relation of $\delta\ddot{w}_{Mj}$ and the structural damping ζ.

4.4. Applicability and accuracy of alternative methods for consideration of vehicle-bridge-interaction

This section aims to give an overview of the applicability and accuracy of the five previously described methods for considering VBI effects in simplified MLM calculations, M1 to M5, as observed in the numerical study.

4.4.1. M1 – Additional mass acc. to ÖBB guidelines [9]

Implementing an additional mass $\Delta\mu$ to MLM calculations as proposed by M1 acc. to the ÖBB guidelines [9] represents an easy-to-handle approach with no need for any vehicle information.

However, in the numerical study described in the previous sections, the application of M1 yield a large number of high values of $\delta\ddot{w}_{M1}$, especially in the case of the Railjet for bridges with a low fundamental frequency ($n_0 \lesssim 12$ Hz, see Fig. 12), while, at the same, also producing a high number of negative and, therefore, unsafe results. According to Fig. 11, bridges with a low mass distribution below the average value of $\overline{\mu} \lesssim 16\,540$ kg m^{-1} are related to a strong over- and underestimation of the maximum acceleration, i. e., very high or negative values of $\delta\ddot{w}_{M1}$. A strong positive correlation between the general effect of VBI and the effect of applying M1 could be observed whereby in cases of a moderate influence of the VBI ($\delta\ddot{w}_{MLM} \lesssim 15$ % see Fig. 10, the acceleration results obtained by applying M1 tend to underestimate the results obtained with the more complex DIM significantly ($\delta\ddot{w}_{M1} < 0$ %).

In conclusion, the alternative method M1 of implementing an additional mass to reflect the impact of vehicle-bridge-interaction performs best for bridges with above-average mass distribution μ (also related to a smaller influence of VBI) and for bridges with large spans $L \gtrsim 20$ m. The recommendation to not apply this method for bridges with short spans ($L < 7$ m) given in [9] could be confirmed since almost exclusively negative values of $\delta\ddot{w}_{M1}$ were calculated for bridges in this range.

4.4.2. M2 - additional damping acc. to EN 1991–2:2003/AC:2010 [1]

The method M2 of considering an additional damping $\Delta\zeta_{M2}$ to consider VBI effects, which must currently be used acc. to EN 1991–2:2003/AC:2010 [1], is also very user-friendly and does not require any vehicle information. It performs similarly to M1 in terms of the number of bridge structures experiencing exceptionally high (insufficiently damped) and negative (excessively damped) values of $\delta\ddot{w}_{M2}$. For structures with particularly wide spans ($L \gtrsim 25$ m), for which the determination function for $\Delta\zeta_{M2}$ by definition results in minimal additional damping, there are correspondingly high structural accelerations that significantly exceed those from DIM calculations and do not represent any improvement compared to the MLM calculation.

In the case of medium spans L, both significant overestimation ($\delta\ddot{w}_{M2} \geq 20$ %, see Fig. 11 for the Railjet) and underestimation of the bridge accelerations ($\delta\ddot{w}_{M2} < 0$ %) are possible. This is possibly related to the fundamental frequency of the bridges since, especially with low fundamental frequencies $n_0 \leq 12$ Hz, large deviations can be observed in the results obtained from MLM and M2 and those generated with the DIM. The results obtained from this numerical study confirm the findings in [3–5].

4.4.3. M3 – Additional damping acc. to Yau et al. [10]

In order to apply method M3 according to [10] and determine the additional damping $\Delta\zeta_{M3}$ more precise knowledge of the vehicle properties is required. The results generated by implementing $\Delta\zeta_{M3}$ are, in the case of the Railjet, apart from the structures with wide spans ($L \gtrsim 25$ m), scarcely better than the results obtained with $\Delta\zeta_{M2}$, whereby the accuracy of method M3 decreases as the influence of the VBI increases (see Fig. 10). In the case of the ICE 4 and the vehicle properties of the powered passenger cars, applying M3 yields accelerations that are significantly too low and, therefore on the unsafe side. When using the unpowered car's vehicle data, the calculation results are much closer to those generated by the more complex DIM. Here, however, the occurrence of many negative results of $\delta\ddot{w}_{M3}$ is noteworthy, which, despite the tendency towards relatively small deviations ($\delta\ddot{w}_{M3} \approx 0$ %), represent acceleration results on the unsafe side.

The deviations of accelerations obtained with the MLM and M3 from those obtained with the DIM observed in the numerical study could be due to the simplified assumptions on which the equivalence system explained in section 2.3.3 is based, such as the assumption of two half

coaches on the structure without taking into account the geometrical compatibility, the neglection of time-dependent wheelset positions, and the limitation to the first vibration mode.

4.4.4. M4 – Additional damping acc. to Stoura and Dimitrakopoulos [11]

Essential vehicle information is also required to apply M4 to [11], namely knowledge of the damping coefficients of the primary stage. This restricts the applicability of M4, as in the examinations described in section 4.2 and the unpowered passenger cars of the ICE 4 with no known damping coefficient c_p. With the time-independent formulation of the determination function for $\Delta\zeta_{M4,i}$, the distance $\overline{d}$ also represents a critical unknown variable, the influence of which should be examined in more detail in further studies.

The acceleration results generated using M4 are, on average, for both trains, closer to those obtained with the DIM than the accelerations resulting from applying both normative methods M1 and M2. The method performs well with steel bridges, while with concrete bridges, where the influence of the VBI is moderate, only insignificant reductions in the maximum accelerations can be generated ($\delta\ddot{w}_{M4} \approx \delta\ddot{w}_{MLM}$, see Fig. 10). Nevertheless, with this method, the most considerable deviations $\delta\ddot{w}_{M4}$ also occur in the case of the Railjet in steel structures with low mass distribution $\mu \leq \overline{\mu}$. In the case of the ICE 4, as with the M3, the accelerations generated are much closer to those obtained with the DIM. The number of structures for which the influence of the VBI is overestimated ($\delta\ddot{w}_{M4} < 0$ %) is, compared to M1 to M3, smaller but still not negligible.

4.4.5. M5 – Additional damping acc. to Glatz and Fink [12]

The additional damping $\Delta\zeta_{M5}$ is with the numerically derived regression functions acc. to M5 [12] easy to determine and independent from vehicle data. However, the applicability of M5 is limited by the scope of the numerical investigations the method is based on, e. g., the restriction to specific trains. The applicability for other trains and coach sequences would have to be examined more closely.

With the trains used in this study, as described in section 3.1, whose properties correspond to those used in [12], M5 produces structural acceleration results with relatively good agreement with those produced using the DIM. This is characterized by a low number of negative and exceptionally high results of $\delta\ddot{w}_{M5}$. As with M4, there is compared to the MLM calculations without additional damping no improvement for concrete structures with rather short spans $L \leq \overline{L}$ and related high natural frequencies n_0, which can be traced back to the upper limit of the frequency-dependent regression functions for determining $\Delta\zeta_{M5}$ in [12] at $n_0 = 10$ to 13 Hz. This limitation is motivated by the mostly negligible influence of VBI for bridges with high natural frequencies observed in [12], which is also observable in this contribution's numerical study. For bridge structures with lower natural frequencies, the application of M5 yields, in the case of the ICE 4, relatively small values of $\delta\ddot{w}_{M5}$ while producing less negative values than M3 and M4.

5. Conclusions and outlook

The effects of applying additional mass or damping on moving load model (MLM) calculations to account for vehicle-bridge-interaction (VBI) following five different approaches are evaluated for 65 existing bridges and two high-speed trains, the Railjet and the ICE 4. The individual results of acceleration peaks are compared with those obtained by applying the more sophisticated DIM of each train, resulting in the comparative value $\delta\ddot{w}$.

In general, the considered bridges that are categorized as steel- or composite structures, bridges with low fundamental frequencies $n_0 \leq 12$ Hz and bridges with low mass distribution μ benefit the most from considering vehicle-bridge-interaction effects by applying the DIM of the vehicle.

The subsequent evaluation allows assessing the benefits of the

different calculation concepts for the additional mass or damping regarding their accuracy and possible applications. For the scope of the previously described investigations, the following conclusions can be drawn:

1. All approaches M1 to M5 yield for the considered bridges, on average, a reduction of acceleration peaks calculated with the MLM, leading to better compliance with results obtained with the detailed interaction model (DIM). However, the different approaches differ in the level and prevalence of particularly strong over- /underestimation of the beneficial effects of VBI.

2. By applying one of the redesigned additional damping methods M3 [10], M4 [11], and M5 [12] to MLM calculations, the acceleration results can reflect the damping influence of VBI on the design-relevant structural accelerations considerably more reliable than by using normative specifications as described in methods M1 [9] and M2 [1].

3. Applying M3, M4, or M5 leads, compared to the normative approaches M1 or M2, in a lower number of bridge structures to an excessive reduction of the acceleration peaks and, therefore, non-conservative results ($\delta\ddot{w} < 0$ %). This does not apply to calculations using M3 and the ICE 4, which tend to overestimate the damping effect of VBI significantly.

4. Furthermore, the observed number of bridges subjected to substantial underestimation of the beneficial effect of VBI ($\delta\ddot{w} \gg 0$ %) and its level is lower if M3 to M5 instead of M1 or M2 is applied.

5. No specific application recommendations can be given for the analytically derived method M3 as described by Yau et al. in [10] since its application leads to strongly divergent outcomes for different train properties. Based on the properties of the ICE 4, it produces, in almost all cases, non-conservative acceleration results. Based on the properties of the Railjet, M3 performs better than the normative M2 as especially bridge structures with medium spans and low natural frequencies are less likely to get overly damped.

6. The analytically derived approach M4 acc. to [11] can only be applied if the vehicle's primary damping coefficient is known. It performs best with bridge structures with medium to high mass distributions. It generally produces less non-conservative (overestimated VBI) accelerations than the normative approaches.

7. The approach acc. to Glatz and Fink [12] performs best for bridge structures with a generally strong impact of VBI and those with spans over average. For both trains, it leads to a low number of excessively damped bridge structures and only few strong underestimations of additional damping due to VBI. This can be explained by the fact that this approach is derived from numerical studies explicitly conducted for both considered high-speed trains. Therefore, further analysis of the performance for deviating train parameters is advised.

Further research incorporating existing research should give closer consideration to the extent of VBI effects on bridge vibrations and, therefore, the benefit of applying one of the methods.

The findings in this contribution are limited to the two considered train configurations, for which the effects of implementing one of the five methods differ, in parts, significantly. Further analysis of the performance of the methods for deviating train parameters is advised. For the two trains considered, the properties of the locomotives and passenger cars (Railjet) or the powered and unpowered cars (ICE 4) differ significantly concerning the car masses (Railjet) and properties of the primary and secondary stages (Railjet and ICE 4) which complicates the application of methods M3 and M4 in particular. The influence of the VBI and the application of the methods examined here to determine the additional damping for trains with similar characteristics of all cars, such as trains with exclusively powered axles (power distribution trains) or articulated trains, should be addressed in further investigations.

The applicability of methods M1 to M5 to other types of trains, such as articulated trains, heavily depends on the different methods'

derivation. The train-independent methods M1 [9] and M2 [1] can be applied to calculations with articulated trains without problems. Since only coupling properties between wheelsets and bogies are included in the derivation of M4 [11] and the additional damping is determined specifically for each individual train in the M5 [12], these two methods can also be easily transferred to other train types. In contrast, the formulation of the additional damping acc. to M3 [10] depends on the underlying model of two consecutive but decoupled bogies, which cannot be directly transferred to a model for articulated trains. The applicability needs to be checked accordingly.

The applicable methods discussed in this article are based on the determination of additional damping or mass contributions from VBI, which consider its influence independent of time over the total duration of the train crossing. However, the influence of VBI depends on the time-variant position of the vehicle axles on the bridge structure, thus leading to different effects with diverging bridge spans and train axle distances (see findings in [32]). The continuous further development of numerical methods for identifying the instantaneous modal frequencies and damping of bridge structures from measured vibration responses, such as those presented by Matsuoka et al. [32] or Yuan et al. [33], enable a more detailed investigation of the time-variant influence of the interaction dynamics between train and bridge structure. Future research activities on the development of simplified methods of considering VBI can make use of such time-dependent analyses of its influence, for example, for verification purposes and differentiated adjustment of the methods to deviating boundary conditions.

Declaration of Competing Interest

The authors declare that they have no known competing financial interests or personal relationships that could have appeared to influence the work reported in this paper.

Data availability

Data will be made available on request.

Acknowledgements

References

[1] CEN European Committee for Standardization. EN 1991-2:2003/AC:2010 Eurocode 1: Actions on structures - Part 2: Traffic loads on bridges(EN 1991-2: 2003/AC:2010).

[2] Liu K, De Roeck G, Lombaert G. The effect of dynamic train–bridge interaction on the bridge response during a train passage. J Sound Vib 2009;325(1-2):240–51.

[3] Doménech A, Museros P. Influence of the vehicle model on the response of high-speed railway bridges at resonance. Analysis of the Additional Damping Method prescribed by Eurocode 1. Proceedings of the 8th International Conference on Structural Dynamics, EURODYN 2011 2011:1273–80.

[4] Arvidsson T, Karoumi R, Pacoste C. Statistical screening of modelling alternatives in train–bridge interaction systems. Eng Struct 2014;59:693–701.

[5] Glatz B, Fink J. Einfluss der Zugmodelle auf die dynamische Antwort von 75 Stahl-, Verbund- und Stahlbetonbrücken Stahlbau 2019;88(5):470–7.

[6] Ribeiro D, Costa B, Cruz L, Oliveira M, Alves V, Montenegro P, et al. Simulation of the Dynamic Behavior of a Centenary Metallic Bridge under Metro Traffic Actions Based on Advanced Interaction Models. Int J Str Stab Dyn 2021;21(04):2150057.

[7] CEN European Committee for Standardization. EN 1990:2002/A1:2005/AC:2010 Eurocode - Basis of structural design(EN 1990:2002/A1:2005/AC:2010).

[8] Doménech A, Museros P, Martínez-Rodrigo MD. Influence of the vehicle model on the prediction of the maximum bending response of simply-supported bridges under high-speed railway traffic. Eng Struct 2014;72:123–39.

[9] ÖBB Infrastruktur AG. Richtlinie für die dynamische Berechnung von Eisenbahnbrücken (RW 08.01.04); 2011.

[10] Yau JD, Martínez-Rodrigo MD, Doménech A. An equivalent additional damping approach to assess vehicle-bridge interaction for train-induced vibration of short-span railway bridges. Eng Struct 2019;188:469–79.

[11] Stoura CD, Dimitrakopoulos EG. Additional damping effect on bridges because of vehicle-bridge interaction. J Sound Vib 2020;476:115294. https://doi.org/10.1016/j.jsv.2020.115294.

[12] Glatz B, Fink J. A redesigned approach to the additional damping method in the dynamic analysis of simply supported railway bridges. Eng Struct 2021;241:112415. https://doi.org/10.1016/j.engstruct.2021.112415.

[13] Matsuoka K, Collina A, Somaschini C, Sogabe M. Influence of local deck vibrations on the evaluation of the maximum acceleration of a steel-concrete composite bridge for a high-speed railway. Eng Struct 2019;200:109736. https://doi.org/10.1016/j.engstruct.2019.109736.

[14] Wu Y-S, Yang Y-B, Yau J-D. Three-Dimensional Analysis of Train-Rail-Bridge Interaction Problems. Veh Syst Dyn 2001;36(1):1–35.

[15] Yang YB, Yau JD, Vehicle-Bridge WYS. Interaction Dynamics: WORLD SCIENTIFIC 2004.

[16] Zhang N, Xia He, Guo W. Vehicle–bridge interaction analysis under high-speed trains. J Sound Vib 2008;309(3-5):407–25.

[17] Dinh VN, Kim KD, Warnitchai P. Dynamic analysis of three-dimensional bridge–high-speed train interactions using a wheel–rail contact model. Eng Struct 2009;31(12):3090–106.

[18] Peixer MA, Montenegro PA, Carvalho H, Ribeiro D, Bittencourt TN, Calçada R. Running safety evaluation of a train moving over a high-speed railway viaduct under different track conditions. Eng Fail Anal 2021;121:105133. https://doi.org/10.1016/j.engfailanal.2020.105133.

[19] Wu Y, Zhou J, Zhang J, Wen Q, Li X. Train-Bridge Dynamic Behaviour of Long-Span Asymmetrical-Stiffness Cable-Stayed Bridge. Shock Vib 2021;2021:1–15.

[20] Eroğlu M, Koç MA, Esen İ, Kozan R. Train-structure interaction for high-speed trains using a full 3D train model. J Braz Soc Mech Sci Eng 2022;44(1). https://doi.org/10.1007/s40430-021-03338-1.

[21] Nguyen K, Goicolea JM, Galbadón F. Comparison of dynamic effects of high-speed traffic load on ballasted track using a simplified two-dimensional and full three-dimensional model. Proceedings of the Institution of Mechanical Engineers, Part F: Journal of Rail and Rapid Transit 2014;228(2):128–42.

[22] Shampine LF, Reichelt MW. The MATLAB ODE Suite. SIAM J Sci Comput 1997;18(1):1–22.

[23] Yang Y-B, Yau J-D, Hsu L-C. Vibration of simple beams due to trains moving at high speeds. Eng Struct 1997;19(11):936–44.

[24] Lei X, Noda N-A. Analyses of dynamic response of vehicle and track coupling system with random irregularity of track vertical profile. J Sound Vib 2002;258(1):147–65.

[25] Sun YQ, Dhanasekar M. A dynamic model for the vertical interaction of the rail track and wagon system. Int J Solids Struct 2002;39(5):1337–59.

[26] Mähr TC. Theoretische und experimentelle Untersuchungen zum dynamischen Verhalten von Eisenbahnbrücken mit Schotteroberbau unter Verkehrslast. Dissertation Wien 2008.

[27] Azimi H. Development of VBI Models with Vehicle Acceleration for Bridge-Vehicle Dynamic Responses. Canada: Montréal; 2011. PhD Thesis.

[28] Frýba L. Vibration of solids and structures under moving loads. Dordrecht: Springer, Netherlands; 2012.

[29] ERRI European Rail Research Institute. ERRI D 214/RP9, Rail bridges for speeds > 200 km/h; 1999.

[30] Firus A, Berthold H, Schneider J, Grunert G. Untersuchungen zum dynamischen Verhalten einer Eisenbahnbrücke bei Anregung durch den neuen ICE 4. In: Baudynamik 2018: VDI Verlag; 2018. p. 233–48. https://doi.org/10.51202/9783181023211-233.

[31] Weisberg S. Applied linear regression. 3rd ed. Hoboken, N.J: Wiley-Interscience; 2005.

[32] Matsuoka K, Kaito K, Sogabe M. Bayesian time–frequency analysis of the vehicle–bridge dynamic interaction effect on simple-supported resonant railway bridges. Mech Syst Sig Process 2020;135:106373. https://doi.org/10.1016/j.ymssp.2019.106373.

[33] Yuan P-P, Zhang J, Feng J-Q, Wang H-H, Ren W-X, Wang C. An improved time-frequency analysis method for structural instantaneous frequency identification based on generalized S-transform and synchroextracting transform. Eng Struct 2022;252:113657. https://doi.org/10.1016/j.engstruct.2021.113657.